MRI Scan Time Reduction through K-Space Data Sharing in Combo Acquisitions with a Spin Echo Sequence

R. Mekle[1], E. X. Wu[2], and A. F. Laine[1, 2]

[1]Department of Biomedical Engineering, Columbia University, New York, USA
[2]Department of Radiology, Columbia University, New York, USA, rm197@columbia.edu

Abstract – **We propose a technique to reduce scan time for magnetic resonance imaging (MRI) through sharing of k-space data between images. As a proof of concept, we ran simulations of MRI experiments based on Bloch equations using a spin echo sequence. We generated images of a realistic brain phantom containing the tissues: white matter, gray matter, and cerebrospinal fluid. A set of k-space data was acquired while varying two acquisition parameters: repetition time (TR) and echo time (TE). This data set was then used to reconstruct multiple images of different contrast. Customized variation of TR and TE allowed us to obtain different contrast weightings of signal values. We present results for 2-contrast and 3-contrast "combo" acquisitions and compare them with images from acquisitions with fixed TR and TE. Scan time reductions of 30%-52% were achieved. Artifacts stemming from non-uniform and tissue-dependent data weighting in the Fourier domain were minimized through systematic optimization of the order of phase encoding and of variation schemes for TR and TE. No obvious degradation of image quality and resolution was observed. In addition, we quantitatively analyzed preservation of contrast, image profiles of sharp tissue boundaries, and signal-to-noise-ratio.**

Keywords – **MRI, combined/combo acquisition, variable acquisition parameter, k-space data sharing, scan time reduction.**

I. INTRODUCTION

Scan time reduction in magnetic resonance imaging (MRI) remains an important issue, especially when considering acquisition of diagnostic images in a clinical setting. Shortening of acquisition times entails reduction of costs and increased patient throughput and comfort. Improvements of scanner hardware over the last twenty years allowed the development of fast acquisition schemes, such as echo planar imaging (EPI) [1], fast spin echo (FSE [2]), and fast gradient echo sequences [3]. Other approaches to scan time reduction include partial Fourier imaging [4], reception of MR signals with multiple coils (SMASH) [5], and traversing k-space on different trajectories than on a Cartesian grid [6]. Most of these ideas attempt to increase the acquisition of data within one sequence cycle, i.e. a larger portion of k-space is sampled before a subsequent rf-excitation. Recently, this concept was also applied to a single-shot spin echo sequence [7]. Despite all the improvements on acquisition speed, one image of a particular contrast at a time is acquired with each sequence. If multiple images of various contrasts are needed, e.g. a T_1- and a T_2-weighted image for clinical diagnosis, image acquisition has to be repeated. The resulting total scan time for all images is then the sum of the scan time for each image with a specific contrast. Moreover, in most cases a new scan setup, such as slice prescription is required to obtain an additional image of a different contrast of exactly the same spatial volume as in preceding scans for a better diagnostic comparison of images.

Our work attempted to eliminate these constraints and to prove the concept of combining the acquisition of images of different contrasts into one acquisition through sharing of k-space data in conventional Fourier encoding.

To generate k-space data for multiple contrasts, the paradigm of fixed TR and TE was replaced by varying these parameters during acquisition of all phase encoding views. Different views in k-space were acquired with different TR and/or TE. Signals for low frequencies (small ky-values) were acquired separately for each image to be reconstructed to preserve contrast, but sharing of high-frequency data led to scan time reductions of 30%-52%. We term our approach "combo acquisition" in contrast to conventional imaging with fixed TR and TE, which we denote by "single acquisition". A similar approach to reduce scan time for a spin echo sequence was presented in [8], but in this work only a T_2–weighted image was reconstructed. In addition, variable TE was previously employed to shorten the echo time for *in vivo* MR microscopy [9] and to analyze the loss of small objects in variable TE imaging [10]. Similarly, TR was varied to optimize magnetic resonance angiography (MRA) [11] and to shorten total acquisition time in spectroscopic imaging [12].

The use of simulations allowed us to investigate the effects of non-steady state effects due to varying TR and to streamline the optimization of our acquisition method. Using a spin echo (SE) sequence simplified simulations and was chosen for a proof of concept, but, in general, our scheme could be extended to other sequences, e.g. FSE.

II. METHODOLOGY

A. Simulation of MRI Acquisition

Acquisition of MR signals was simulated by solving the Bloch equations [13] in the rotating frame of reference for each point of an object. Objects were generated as phantom data with voxels modeled as point sources at locations *(x, y, z)* with physical properties, such as spin density, gyromagnetic ratio, and relaxation times.

The phenomenological Bloch equations provide a classical description of the time evolution of a magnetization vector $\vec{M} = \left(M_x, M_y, M_z \right)^T$ in the presence of a magnetic field including relaxation effects:

$$\frac{d\vec{M}}{dt} = \gamma \vec{M} \times \vec{B}_{ext} + \frac{1}{T_1}\left(M_0 - M_z \right)\hat{z} - \frac{1}{T_2}\vec{M}_\perp , \qquad (1)$$

where γ is the gyromagnetic ratio, $\vec{B}_{ext}$ an external magnetic field, M_0 the equilibrium magnetization of the system, M_z the magnetization along the z-axis, $\vec{M}_\perp$ the magnetization vector in the transverse *(x, y-)* plane, and T_1, T_2 are the

longitudinal and transverse relaxation time, respectively. In general, these equations hold for systems with weakly coupled spins. Using Bloch equations to predict MR signals was also employed in [14] and [15].

MRI signals were computed by sampling the transverse magnetization in the rotating frame of reference, which is proportional to the signal from data acquisition plus demodulation in a real MRI experiment [16]. For our combo acquisition, TR and TE were assigned values according to desired variations of these parameters over all sequence cycles. For each sequence cycle a timing protocol was set up that determined timing, durations, and amplitudes of applied magnetic fields, such as gradients and rf-pulses. Analytical solutions of the Bloch equations that exist for special cases of applied magnetic fields, e.g. gradient fields only, were used to compute the evolution of the magnetization, whenever applicable. Image reconstruction was carried out by inverse Fourier transform of the MR signal.

For our simulations we used the realistic brain phantom model from the McConnell Brain Imaging Centre (BIC) of the McGill University in Montreal [17]. We selected the tissues white matter (WM), gray matter (GM), and cerebrospinal fluid (CSF) and modeled spin populations as magnetization vectors of object points. Each object point had associated with it a location (x, y, z), and values for spin density ρ, gyromagnetic ratio γ, and relaxation parameters T_1 and T_2. Moreover, the same location or voxel could have multiple tissue contributions with different physical parameters. The contribution of each tissue to a specific voxel was indicated by voxel fractions v_i with $v_i \in [0,1]$, and $\sum_i v_i = 1$ for each voxel [17], [15]. Simple test phantoms were generated with homogeneous object points, i.e. $v_i = 1, \forall v_i$. Parameters characterizing the physical properties of the tissues WM, GM, and CSF for our experiments were obtained form the literature [16]. The gyromagnetic ratio γ was set to 42.576 MHz/T for all object points, since only proton imaging was considered. Phantom data of in-plane (x, y)-resolutions of 0.1cm x 0.1 cm or 0.1cm x 0.2 cm respectively were generated. For simplicity, it was assumed that phantom models were uniform along the z-direction for the entire selected slice thickness.

B. Optimization Strategy

Varying acquisition parameters TR and TE over all phase encoding views of a particular image leads to non-uniform and tissue-dependent data weighting in k-space. This is similar to data acquisition with multiple echoes, e.g. using a FSE sequence [2]. Non-uniform data weighting in the Fourier domain inevitably yields artifacts in the image domain. Our goal was to optimize our combo acquisitions to preserve contrast and to minimize artifacts in the resulting images.

For contrast preservation the zero phase encoding step for each image in a combined acquisition was acquired with the same settings for TR and TE as used to obtain a specific contrast in a single acquisition. In general, most of the variation of TR and TE to obtain different contrast weighting

occurred during the acquisition of high frequency views. $Ny=256$ phase encoding views were used to encode an image, and we divided this number into segments of 64 or 32. We either repeated the acquisition of a segment for each image or shared its data between multiple images. An example of such a phase encoding (PE) scheme for a 2-contrast combo acquisition is shown in Fig. 1, where is also indicated which segments of k-space are used to reconstruct a T_1- and a T_2-weighted image, respectively. Stepping through all phase encoding numbers was carried out in zigzag fashion.

To guide the design of variation schemes for TR and TE, we acquired data with phase encoding set to zero for a single object point separately for each tissue. We plotted signal magnitudes (levels) of all tissues for $kx=0$ for each image over all sequence cycles (PE numbers ky) to visualize the distribution of signal levels according to variation of TR and TE. Curves for TR and TE were modified, where possible, to preserve the order of signal levels for a particular contrast, e.g. $M_\perp^{WM} > M_\perp^{GM} > M_\perp^{CSF}$ for a T_1-weighted image, and to minimize discontinuities between signal levels for different segments of views. An example for the results of these experiments for a 2-contrast combo acquisition with linear variation of TR and TE is shown in Fig. 2.
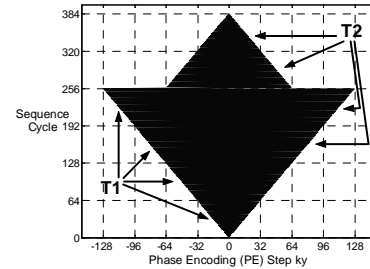

Fig. 1. Phase encoding (PE) scheme for 2-contrast combo acquisition (T_1-T_2) with 384 sequence cycles. Arrows indicate segments for reconstruction of a T_1- and a T_2-weighted image.
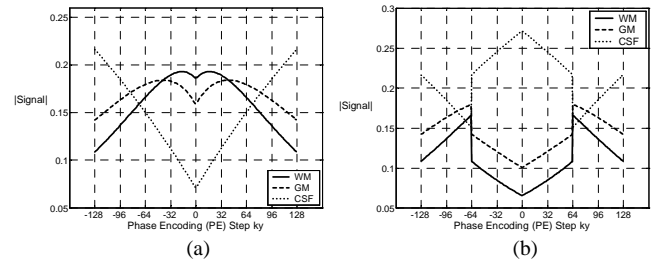

Fig. 2. Signal levels according to linear variation of TR and TE for tissues WM, GM, and CSF for (a) a T_1-, and (b) a T_2-weighted image of a 2-contrast combo acquisition.

III. RESULTS

We present results for 2-contrast and 3-contrast combo acquisitions and compare these images with those from single acquisitions in terms of image contrast, quality, and resolution. All presented images are magnitude images. If not stated otherwise, $Nx=256$ frequency encoding steps, $Ny=256$ phase encoding (PE) steps, and $NEX=1$ averages were used.

A. Images from Single (Standard) Acquisitions

Images of three different contrasts (T_1-, proton density (PD)-,

and T_2-weighted) were acquired using a single TR and a single TE. The choices of acquisition parameters TR and TE for these contrasts are summarized in Table I.

TABLE I
ACQUISITION PARAMETERS TR AND TE FOR THREE DIFFERENT CONTRASTS

Contrast	TR (ms)	TE (ms)
T_1	500	20
PD	2500	20
T_2	2500	150

B. Images from 2-Contrast Combo Acquisition

Our first attempts to share k-space data between two images focused on a combined acquisition of a T_1- and a T_2-weighted image, since these two contrasts are of greatest importance in clinical diagnosis. Using the PE scheme shown in Fig. 1 we varied TR and TE linearly over all views from minimum values, $TR_{min}=500$ms and $TE_{min}=20$ms, to maximum values $TR_{max}=2500$ms and $TE_{max}=150$ms, respectively. Both images exhibited severe artifacts, which were attributed to the fact that by changing TE linearly, signal levels ($\propto$ transverse magnetization) for WM and GM decreased fast, whereas signal levels for CSF were less sensitive to changes of TE due to its long T_2. Better results were obtained, when using sigmoidal ($f(t) = (1+e^{-t})^{-1}$) and sinusoidal functions to vary TR and TE. One choice of variation schemes that yielded images without major artifacts is shown in Fig. 3. The corresponding images are presented in Fig. 4. The T_1-weighted image showed only minor CSF brightening, and in the T_2-weighted image only minor ringing within the areas of WM and GM was left.
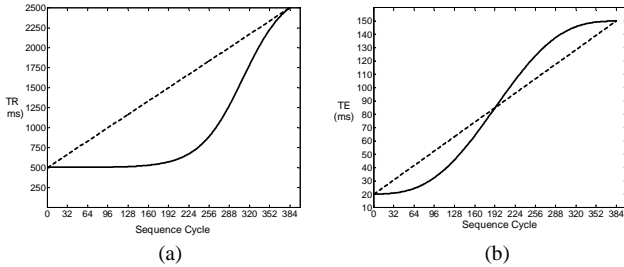

Fig. 3. Optimized variation scheme for TR and TE for 2-contrast combo acquisition: (a) sigmoidal curve for TR and (b) sinusoidal curve for TE. Linear curves for TR and TE are included as dashed lines for comparison.
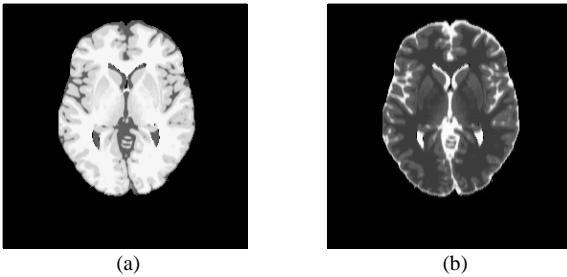

Fig. 4. Images from 2-contrast combo acquisition using the variation scheme of Fig. 3 with scan time reduction of 52%: (a) T_1- and (b) T_2-weighted image.

Aside from a combining the acquisition of a T_1- and a T_2-weighted image, k-space data sharing was also applied for images of T_1- and PD-contrast or of PD- and T_2-contrast. Similar or even better results were obtained, since for those cases only one of the acquisition parameters had to be varied.

C. Images from 3-Contrast Combo Acquisition

Initially, we shared views with $|ky|>64$ among the three images of different contrasts causing major artifacts. We adjusted our approach by extending results from 2-contrast combo acquisitions to 3-contrasts by appending additionally acquired parts of k-space data for the third image. We systematically determined how large of a change in signal level for each of the three tissues for an image of a particular contrast was tolerable and when it led to major artifacts. In addition, we favored schemes that resulted in larger scan time reduction. A set of images for a specific variation of TR and TE is shown in Fig. 5 together with corresponding images from single acquisitions. As seen in Fig. 5, images from the combo acquisition had good contrast definition and did not exhibit any major artifacts. Especially, the T_1- and the T_2-weighted images were very similar to their counterparts from single acquisitions.
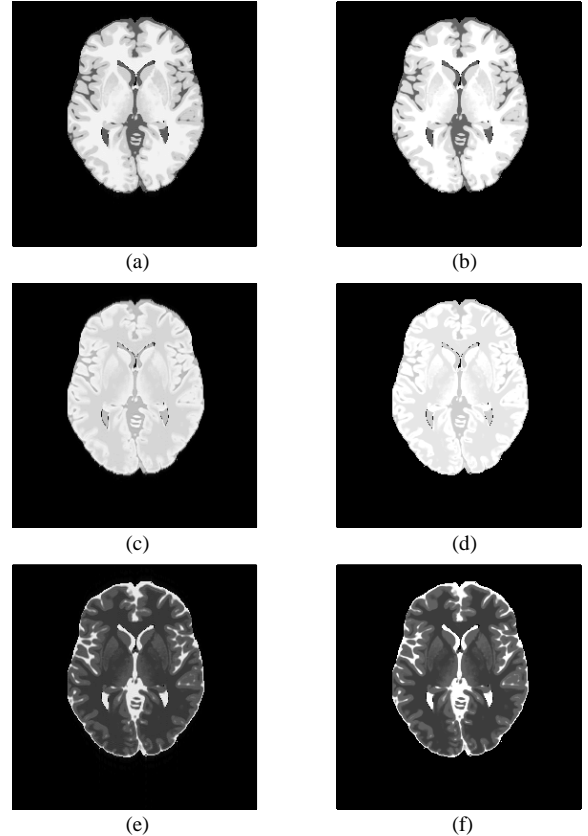

Fig. 5. Images of three different contrasts, T_1-, PD-, and T_2-weighted: Images in (a), (c), and (e) from 3-contrast combo acquisition and images in (b), (d), and (f) from single acquisitions with parameters from Table I. Scan time was reduced by 31.5% with the combo acquisition.

D. Scan Time Reduction

Scan time reduction for the images from the 2-contrast combo acquisition in Fig. 4 was *52%*. Similar values were obtained using other variation schemes for TR and TE and for T_1-PD combo acquisitions. For *PD-T_2* combo acquisitions scan times could be reduced by only *25%* due to acquisition with a long TR. Images obtained with a 3-contrast combo acquisition shown in Fig. 5 were acquired with *31.5%* less scan time

compared to single acquisition. Larger scan time savings for three contrasts were achieved with different curves for TR and TE. In these cases, image contrast or quality was less good.

E. Filtering

To correct for different data weighting in k-space, we applied filters derived from the distribution of signal levels over all PE numbers of an image. In general, filtering had limited benefits: some artifacts were removed, while others were amplified. Tissue-selective filters would be needed to compensate for tissue-dependent signal levels.

IV. DISCUSSION

In our experiments, many variation schemes for TR and TE were tested to study over which PE numbers changes in signal levels degraded the resulting image most. In summary, changing the signal level over the highest spatial frequency data with respect to phase encoding ($|ky|>96$) entailed less image degradation than over k-space regions of lower frequencies as expected. In addition, the impact of signal level variations depended on the signal level of the tissue itself. The two brightest tissues of the resulting image of a specific contrast, e.g. WM and GM in a T_1-weighted image, were usually more prone to show artifacts, when their signal levels were varied, than the tissue with the lowest image intensity. To further assess results from combo acquisitions, we analyzed preservation of contrast, image profiles across sharp tissue boundaries, and the signal-to-noise-ratio (SNR) of each image.

To obtain a measure for contrast we computed ratios of average image intensities in selected regions-of-interest (ROIs) of homogeneous tissue content. Ratios were computed for all tissue combinations (WM-GM, WM-CSF, and GM-CSF). The results of these measurements for images from single and combo acquisitions were nearly identical. Thus, no significant contrast degradation was observed.

Image profiles across sharp tissue boundaries (edges) were generated from images of a phantom that consisted of two adjacent rows of three consecutive homogeneous tissue blocks of size 60x30 units along x and y. The distribution of tissues WM, GM, and CSF over the six blocks was chosen to obtain profiles along the y-axis in reconstructed images for all tissue combinations. Only minor Gibbs ringing across edges was found for images from combo acquisitions compared to profiles from single acquisitions.

Finally, we added Gaussian white noise independently to the real and imaginary parts of k-space data and computed the SNR in the resulting magnitude image. Noise was zero mean, had either a fixed or bandwidth dependent variance, and was measured in a ROI outside of the brain area. Signal was computed as average image intensity of a ROI of homogeneous WM. SNRs for noise with fixed variance were the same for images from combo and single acquisitions. For bandwidth dependent noise, SNRs improved for images of combo acquisitions that were partially acquired with longer TR than in a single acquisition allowing a smaller sampling bandwidth. In turn, the SNR was slightly lower, when parts of k-space were acquired with shorter TR.

V. CONCLUSION

Simulations of MRI experiments based on Bloch equations were run to test the concept of k-space data sharing between images of multiple contrasts in combined/combo acquisitions. Scan time reductions of *30%-52%* were obtained compared to single acquisitions. In practice, such a combo acquisition can further save scan time by eliminating the need for setting up acquisition of various contrasts individually. Image contrast was well preserved, and artifacts were significantly suppressed through systematic optimization of phase encoding order and variation schemes for acquisition parameters TR and TE.

REFERENCES

[1] P. Mansfield, A. A. Maudsley, and T. Baines, "Fast scan proton density imaging by NMR," *J. Phys. E: Scient. Instrum.*, vol. 9, pp. 271, 1976.

[2] J. Listerud, S. Einstein, E. Outwater, and H. Y. Kressel, "First principles of fast spin echo," *Magnetic Resonance Quarterly*, vol. 8, pp. 199-244, 1992.

[3] P. van der Meulen, J. P. Groen, and J. J. Cuppen, "Very fast MR imaging by field echoes and small angle excitation," *Magnetic Resonance Imaging*, vol. 3, pp. 297-9, 1985.

[4] E. M. Haacke, E. D. Lindskog, and W. Lin, "A fast, iterative, partial-Fourier technique capable of local phase recovery," *Journal of Magnetic Resonance*, vol. 92, pp. 126-45, 1991.

[5] D. K. Sodickson and W. J. Manning, "Simultaneous acquisition of spatial harmonics (SMASH): fast imaging with radiofrequency coil arrays," *Magnetic Resonance in Medicine*, vol. 38, pp. 591-603, 1997.

[6] D. B. Twieg, "The k-trajectory formulation of the NMR imaging process with applications in analysis and synthesis of imaging methods," *Medical Physics*, vol. 10, pp. 610-21, 1983.

[7] J. H. Duyn, "High-speed interlaced spin-echo magnetic resonance imaging," *Magnetic Resonance in Medicine*, vol. 43, pp. 905-8, 2000.

[8] R. K. Butts, F. Farzaneh, S. J. Riederer, J. N. Rydberg, and R. C. Grimm, "T2-weighted spin-echo pulse sequence with variable repetition and echo times for reduction of MR image acquisition time," *Radiology*, vol. 180, pp. 551-6, 1991.

[9] H. K. Song and F. W. Wehrli, "Variable TE gradient and spin echo sequences for in vivo MR microscopy of short T2 species," *Magnetic Resonance in Medicine*, vol. 39, pp. 251-8, 1998.

[10] R. T. Constable and J. C. Gore, "The loss of small objects in variable TE imaging: implications for FSE, RARE, and EPI," *Magnetic Resonance in Medicine*, vol. 28, pp. 9-24, 1992.

[11] J. A. Tkach, W. Lin, J. J. J. Duda, E. M. Haacke, and T. J. Masaryk, "Optimizing three-dimensional time-of-flight MR angiography with variable repetition time," *Radiology*, vol. 191, pp. 805-11, 1994.

[12] B. Kuhn, W. Dreher, D. G. Norris, and D. Leibfritz, "Fast proton spectroscopic imaging employing k-space weighting achieved by variable repetition times," *Magnetic Resonance in Medicine*, vol. 35, pp. 457-64, 1996.

[13] F. Bloch, "Nuclear induction," *Physical Review*, vol. 70, pp. 460-74, 1946.

[14] J. Bittoun, J. Taquin, and M. Sauzade, "A computer algorithm for the simulation of any nuclear magnetic resonance (NMR) imaging method," *Magnetic Resonance Imaging*, vol. 2, pp. 113-20, 1984.

[15] R. K. Kwan, A. C. Evans, and G. B. Pike, "MRI simulation-based evaluation of image-processing and classification methods," *IEEE Transactions on Medical Imaging*, vol. 18, pp. 1085-97, 1999.

[16] E. M. Haacke, R. W. Brown, M. R. Thompson, and R. Venkatesan, *Magnetic Resonance Imaging: Physical Principles and Sequence Design*. New York: J. Wiley & Sons, 1999.

[17] D. L. Collins, A. P. Zijdenbos, V. Kollokian, J. G. Sled, N. J. Kabani, C. J. Holmes, and A. C. Evans, "Design and construction of a realistic digital brain phantom," *IEEE Transactions on Medical Imaging*, vol. 17, pp. 463-8, 1998.